Supporting Information

Wu et al. 10.1073/pnas.1114117109

SI Materials and Methods

Cloning, Expression, and Purification of Human HAT1. A DNA fragment encoding the acetyltransferase domain of human histone acetyltransferase 1 (HAT1) (residues 22–341) was amplified by PCR and subcloned into pET28a-LIC vector, downstream of the poly-histidine coding region. Human HAT1 acetyltransferase domain was overexpressed in *Escherichia coli* BL21 (DE3) codon plus RIL strain (Stratagene) by addition of 1 mM isopropyl-1-thio-D-galactopyranoside and incubated overnight at 15 °C. Harvested cells were resuspended in 50 mM sodium phosphate buffer (pH 7.4), supplemented with 250 mM NaCl, 5 mM imidazol, 2 mM β-mercaptoethanol, and 5% (vol/vol) glycerol. The cells were lysed by passing through a microfluidizer (Microfluidics) at 20,000 psi. After clarification of the crude extract by high-speed centrifugation, the lysate was loaded onto a 5-mL HiTrap chelating column (GE Healthcare), charged with Ni^{2+}. The column was washed with 10 column volumes of 20 mM Tris·HCl buffer (pH 8.0) containing 250 mM NaCl, 50 mM imidazole, and 5% glycerol, and the protein was eluted with 20 mM Tris·HCl buffer (pH 8.0), 250 mM NaCl, 250 mM imidazole, and 5% glycerol. The protein was loaded on a Superdex200 column (26 × 60) (GE Healthcare), equilibrated with 20 mM Tris·HCl buffer (pH 8.0) and 150 mM NaCl. Thrombin (Sigma) was added to combined fractions containing HAT1 to remove the His-tag. The protein was further purified to homogeneity by ion-exchange chromatography. All site-directed mutants of HAT1 described in this work were generated by the QuikChange site-directed mutagenesis kit (Stratagene). The entire coding sequence of each of the HAT1 mutants was verified by DNA sequencing to ensure that no other mutations were introduced during PCR. All HAT1 mutant proteins were purified as described above before assays.

Protein Crystallization, Data Collection, and Structure Determination. Purified HAT1 protein (10 mg/mL) was complexed with acetyl coenzyme A (AcCoA) (Sigma) and histone H4 peptide (amino acids 1–20 of H4, synthesized at Tufts University Core Facility) at a 1:10:5 molar ratio of protein:AcCoA:H4 and crystallized using the sitting drop vapor diffusion method by mixing 1 μL of protein solution with 1 μL of the reservoir solution containing 12% PEG 20,000 and 0.1 M MES-NaOH (pH 6.0). Crystals were soaked in the corresponding mother liquor supplemented with 20% glycerol as cryoprotectant before freezing in liquid nitrogen. Cysteine alkylation was required to improve crystal quality in our crystal optimization trials. A 1-M stock solution of iodoacetamide (Sigma) was prepared immediately before use and added to purified HAT1 at a 1:30 molar ratio of HAT1:iodoacetamide and incubated in dark at room temperature for 30 min. The reaction mixture was then passed through a gel-filtration column wrapped in foil to remove free iodine. Our success in obtaining the X-ray crystal structure of HAT1 bound to acetyl-CoA and the H4 peptide was also based on our extensive crystallization trials of the complex at low pH (5.0–6.0); in this condition, the enzyme was least active and had a short crystallization time (usually overnight). X-ray diffraction data were collected at 100 K at beamline ×12B of the National Synchrotron Light Source at Brookhaven National Laboratory. Data were processed using the HKL-2000 suite (1). The structure of the acetyltransferase domain of HAT1 was solved by molecular replacement using the program MOLREP (2). The crystal structure of yeast HAT1 (Protein Data Bank code 1BOB) (3) was used as the search model. ARP/wARP (4) was used for automatic model building. Refmac (5) was used for structure refinement. The graphics program COOT (6) was used for model building and visualization. Crystal diffraction data and refinement statistics for the structure are presented in Table S1.

HAT1 Acetyltransfer Assays. HAT1 histone acetyltransferase activity was monitored by using fluorescent histone acetyltransferase assay (7). Briefly, CoA generated by the HAT assay reacted with the sulfhydryl-sensitive dye 7-diethylamino-3-(49 maleimidylphenyl)-4-methylcoumarin (cpm) (Sigma), yielding an adduct that was monitored continuously at Ex_{max} = 390 nm and Ex_{max} = 469 nm using a Safire microplate reader (Tecan) to determine the initial rate of the reaction and activity at a single time point. Assays were performed in a mixture of 100 mM Tris·HCl (pH 8.5), 0.01% Igepal, and 0.01% alkylated BSA (Sigma) at 25 °C in triplicates using a 96-well black Costar microplate. Aliquots (50 μL) of the reaction mixture (enzyme, AcCoA, H4) were quenched with 50 μL of ice-cold isopropanol and then mixed with 100 μL of 25 μM cpm in 100 mM Tris·HCl (pH 8.5) and 1% Igepal solution and allowed to react in darkness for 10 min prior to reading. In all our assays, human HAT1 fragment (residues 22–341) was used unless otherwise stated.

Substrate H4 constants were determined by titrating peptide from 0.1 to 500 μM with AcCoA concentration fixed at a saturating concentration of 50 μM. To determine the constants for AcCoA, concentrations were varied from 0.1 to 120 μM with H4 concentration fixed at a saturating concentration of 2 mM. Enzyme concentration was fixed at 0.05 μM. Fluorescence data were collected and converted to the concentration of CoA using the mean conversion factor calculated from the standardization curve. The rate constant k_{cat} and K_m for substrate H4 and AcCoA were determined using the following equations:

$$v = V_{max} \bullet [S]/(K_m + [S]) \quad \textbf{[S1]}$$

$$V_{max} = k_{cat}[E]_0, \quad \textbf{[S2]}$$

where $[E]_0$ is the initial concentration of the substrate and v is the initial rate.

The pH rate profiles for wild-type and mutant HAT1 proteins were determined under a saturating substrate condition of 50 μM AcCoA and 0.05 μM HAT1, and H4 peptide concentration varied from 0.1 to 500 μM. The k_{cat} and K_m were determined at a pH range from 6.0 to 10.5. To maintain a constant ionic strength, three-component buffer mixtures were used (50 mM N-(2-Acetamido)-2-aminoethanesulfonic acid, 25 mM Tris, 25 mM ethanolamine) (8).

The relative abundance of unmodified and modified H4 peptides at different time points was analyzed by mass spectrometry. Reaction solution contained 0.5 μM of HAT1, 100 μM of histone H4 peptide, and 100 μM of AcCoA in the reaction buffer [20 mM Hepes-NaOH (pH 7.4), 100 mM NaCl]. At a certain time point, 20 μL of the reaction mixture was transferred to another tube and mixed with 20 μL of ice-cold isopropanol.

1. Otwinowski Z, Minor W (1997) Processing of X-ray diffraction data collected in oscillation mode. *Methods Enzymol* 276:307–326.

2. Vagin A, Teplyakov A (1997) MOLREP: An automated program for molecular replacement. *J Appl Cryst* 30:1022–1025.

3. Dutnall RN, Tafrov ST, Sternglanz R, Ramakrishnan V (1998) Structure of the histone acetyltransferase Hat1: A paradigm for the GCN5-related N-acetyltransferase superfamily. *Cell* 94:427–438.
4. Perrakis A, Harkiolaki M, Wilson KS, Lamzin VS (2001) ARP/wARP and molecular replacement. *Acta Crystallogr D Biol Crystallogr* 57:1445–1450.
5. Murshudov GN, Vagin AA, Dodson EJ (1997) Refinement of macromolecular structures by the maximum-likelihood method. *Acta Crystallogr D Biol Crystallogr* 53:240–255.
6. Emsley P, Cowtan K (2004) Coot: Model-building tools for molecular graphics. *Acta Crystallogr D Biol Crystallogr* 60:2126–2132.
7. Trievel RC, Li FY, Marmorstein R (2000) Application of a fluorescent histone acetyltransferase assay to probe the substrate specificity of the human p300/CBP-associated factor. *Anal Biochem* 287:319–328.
8. Ellis KJ, Morrison JF (1982) Buffers of constant ionic strength for studying pH-dependent processes. *Methods Enzymol* 87:405–426.

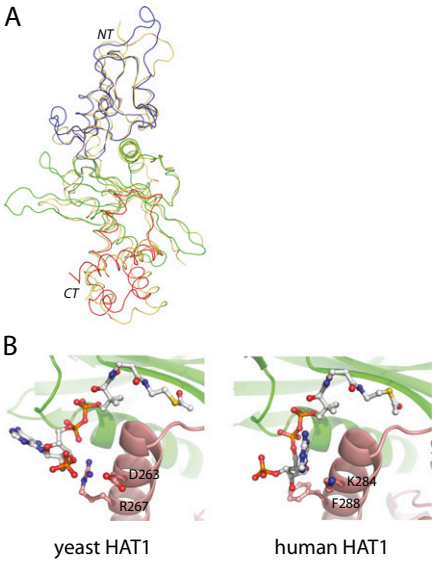

Fig. S1. Comparison of yeast and human HAT1 structures. (*A*) The two structures are shown in ribbon representations. The three domains in human HAT1 structure are blue, green, and red. The yeast structure is yellow. (*B*) Comparison of the binding mode of AcCoA in yeast and human HAT1. The structures of yeast (*Left*) and human (*Right*) HAT1 are shown in cartoon representation. AcCoA and active-site residues critical for the AcCoA-binding mode are shown in stick-and-ball representation.

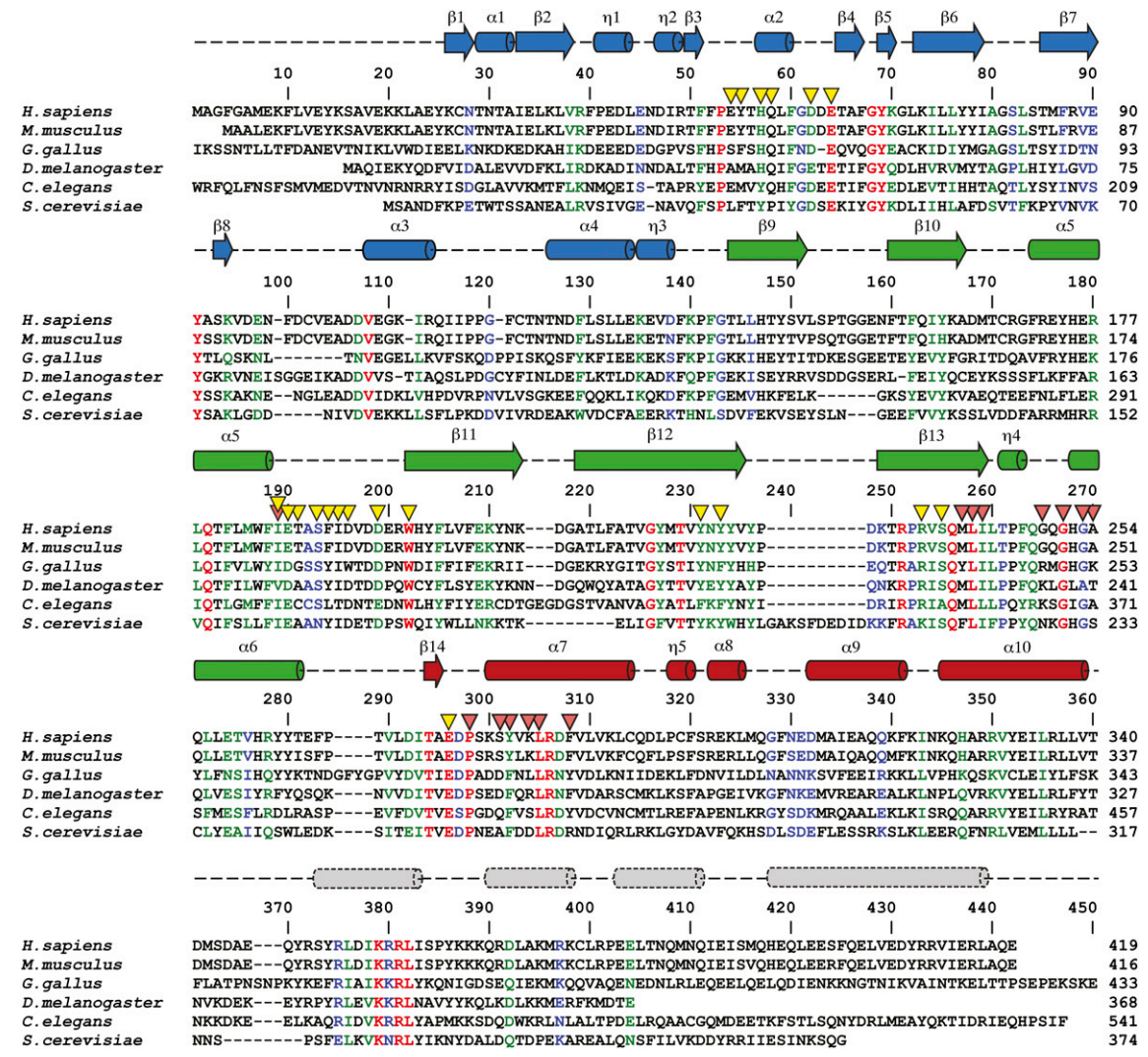

Fig. S2. Structure-based multiple sequence alignment of representative members of the HAT1 family. Identical residues, highly similar, and similar residues are red, green, and blue, respectively, in the alignment. Secondary structure elements of human HAT1 are assigned by the PROCHECK program (1) and are shown above the sequences: the helices are shown as cylinders, and the strands are shown as arrow bars. The residues interacting with AcCoA are labeled with red triangles; the residues involved in H4 binding are labeled with yellow triangles. The three domains in human HAT1 are blue, green, and red, respectively. The predicted secondary structure of the C terminus of HAT1, which is not included in the structure, is gray. The alignment was generated using Clustal W (2) assisted with hand fittings. The sequences shown are from *Homo sapiens* (NP_003633); *Mus musculus* (NP_080391); *Gallus gallus* (Q869 × 7, 4 amino acids truncated from the N terminus, 33 amino acids truncated from C terminus); *Drosophila melanogaster* (Q9VNI2); *Caenorhabditis elegans* (Q21484, 120 amino acids truncated from the N terminus); and *Saccharomyces cerevisiae* (Q12341).

1. Laskowski RA, MacArthur MW, Moss DS, Thornton JM (1993) PROCHECK: A program to check the stereochemical quality of protein structures. *J Appl Cryst* 26:283–291.
2. Thompson JD, Higgins DG, Gibson TJ (1994) CLUSTAL W: Improving the sensitivity of progressive multiple sequence alignment through sequence weighting, position-specific gap penalties and weight matrix choice. *Nucleic Acids Res* 22:4673–4680.

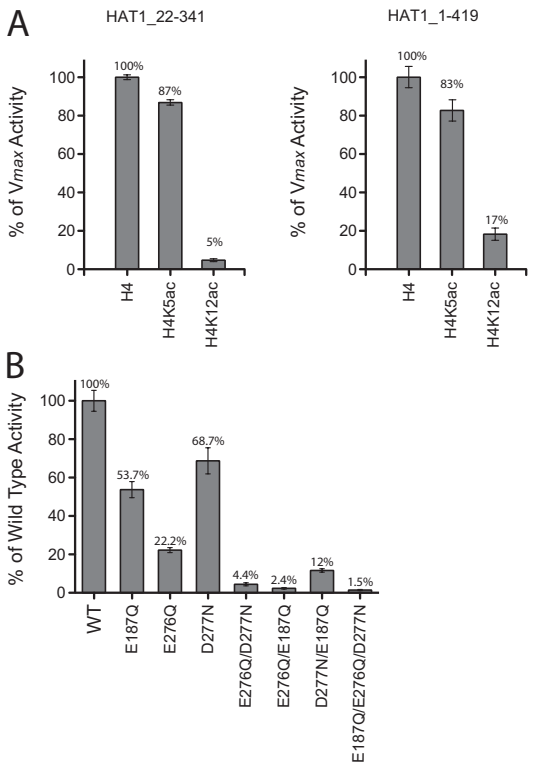

Fig. S3. Enzymatic activity of HAT1. (*A*) Enzymatic activity of HAT1 for different substrates. The spikes represent HAT1 activity toward the substrates H4K5Ac and H4K12Ac with relation to the unmodified peptide H4 measured via steady-state kinetic analysis. The graph for (*Left*) HAT1 (22-341). (*Right*) HAT1 (1-419). (*B*) Enzymatic activity of HAT1 mutants. Shown are the spikes representing activity of HAT1 (22-341) mutants with relation to wild type measured at a fixed concentration of wild-type and mutant HAT1 proteins of 1 μM incubated with substrates (100 μM H4 and 50 μM AcCoA) for 15 min.

Table S1. Crystallography data and refinement statistics

PDB ID code	2P0W
Data collection	
Space group	$P2_12_12$
Cell dimensions	
a, *b*, *c* (Å)	116.56, 155.43, 53.62
α, β, γ(°)	90, 90, 90
Resolution (Å)	100.00–1.90 (1.94–1.90)*
Measured reflections	346,153
Unique reflections	76,880
R_{merge}	10.0 (68.1)
$I/\sigma I$	8.6 (1.6)
Completeness (%)	99.0 (96.3)
Redundancy	4.5 (3.9)
Refinement	
Resolution (Å)	47.35–1.90
No. reflections (test set)	68,545 (3,584)
R_{work}/ R_{free} (%)	18.2/22.8
No. atoms	
Protein	5,509
Cofactor	107
H4 peptide	105
Water	782
B-factors (Å^2)	
Protein	17.8
Cofactor	30.7
H4 peptide	24.8
Water	31.0
rmsd†	
Bond lengths (Å)	0.015
Bond angles (°)	1.43
Ramachandran plot % residues	
Favored	91.2
Additional allowed	8.8
Generously allowed	0
Disallowed	0

*Values in parentheses are for the highest resolution shell.
†Root mean square deviation.